Eur. Phys. J. AP **5**, 257–267 (1999)

THE EUROPEAN PHYSICAL JOURNAL APPLIED PHYSICS

Computation of induction machine inductances for extended analytical modeling accounting for saturation

B. Lemaire-Semail[1,a], J.P. Louis[2], and F. Bouillault[3]

[1] L2EP[b], École Centrale de Lille, B.P. 48, 59651 Villeneuve d'Ascq, France
[2] LESiR[c], ENS de Cachan, 61 avenue du Président Wilson, 94235 Cachan, France
[3] LGEP[d], ESE, plateau du Moulon, 91192 Gif-sur-Yvette, France

Received: 15 December 1997 / Revised: 30 September 1998 / Accepted: 15 December 1998

Abstract. In this paper, finite element method is used to compute inductance parameters of a squirrel cage induction machine. To take into account saturation effect, saturated equivalent parameters are introduced, which depend on the instantaneous value of the magnetising current. For a balanced induction machine, the particular inductance behaviors allow straightforward flux expressions without any cross saturation effect. Moreover, these expressions are explained thanks to an extended analytical approach considering a magnetic saliency phenomenon by a second order air-gap permeance. A simple way of transformation ratio and leakage inductance computation is also deduced. The numerical results show the compatibility between finite element approach and extended analytical Park's method. Besides, two operating points (at no load and for nominal speed) studied by the both methods give very closed results.

PACS. 07.05.Tp Computer modeling and simulation – 07.50.-e Electrical and electronic components, instruments, and techniques

1 Introduction

One of the main concern for induction machine control or modeling deals with parameter identification. Effectively, especially for squirrel cage motors, as very few variables are measurable, the machine becomes difficult to be modelled.

The accuracy of parameter estimate may often improve the control results; despite adaptive control laws are successful to cope with modeling uncertainties, the right knowledge of parameters *a priori* is interesting yet. Many identification methods are available for induction machine characterisation [1,2]. We propose here to apply finite element method (FEM) to the computation of induction machine inductances, so as to obtain the values corresponding to rated flux level, but also to determine their evolution law, accounting for saturation effect. For this approach, we have used the method already developed for synchronous machine identification, with the idea of saturated equivalent inductances. In the first part of the paper, we shall explain the saturated inductance meaning as well as the computation assumptions for an induction machine. In the second part, the interesting results obtained from FEM will be used to elaborate an analytical approach accounting for saturation effect; for that aim, a variable air-gap permeance is introduced. Analytical modeling simulation and FEM results are quite closed, showing the compatibility of the both approaches. Then, some remarquable features will be highlighted about the flux expressions, allowing transformation coefficient and leakage inductance value computation. At last, the extended analytical modeling will be checked for no load and nominal load operating point.

[a] e-mail: `betty.semail@eudil.fr`
[b] UPRES 2697
[c] UPRES A CNRS 8029
[d] UMR CNRS 8507

2 Saturated inductances

2.1 Definition

Speaking of inductances and saturation effect seems to be strange because the inductance concept means a linear relation between magnetic flux and electric current. Obviously, this condition fails when saturation occurs. Then, saturated inductances must be considered as an extended definition of the flux-current function, non linear, depending on flux or current.

2.2 Finite element computation assumptions

First, we suppose that the geometry of the studied devices is available for 2D computation. There would have no change about the principle in 3D case except in flux-vector potential relation.

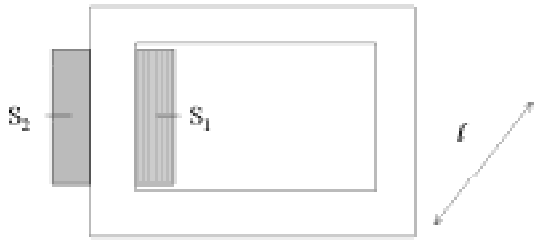

Fig. 1. An example of electromagnetic device.

Magnetic device example

Let us consider a simple example of a single coil around a saturable magnetic core (Fig. 1). From magnetostatic FEM computation with several enforced current values, the magnetic flux φ through one turn is deduced from the following equation (1):

$$\varphi = \iint B \mathrm{d}s = \int A \mathrm{d}l. \tag{1}$$

An average value of A, the magnetic vector potential, is considered over the coil section area: respectively $\langle A \rangle_1$ and $\langle A \rangle_2$ over S_1 and S_2. So the flux φ is computed as:

$$\varphi = \mathcal{I}(\langle A \rangle_1 - \langle A \rangle_2) \tag{2}$$

where $\mathcal{I}$ is the device length. By that way, the main flux is concerned as well as the leakage flux eventually. Noting i the current flowing through the coil, the computed inductance φ/i decreases as the enforced current rises because of saturation effect.

The approach is quite similar for electric machine inductance computation; however, as several coils exist in such devices, the magnetic state may depend on different variables.

Synchronous machine

Many studies have dealt with finite element computation of synchronous machine inductances [3,4]. In that case, the magnetic state of the machine depends on several electromagnetic variables. The exciting field is certainly the most important and its influence is also bounded to mechanical saliency. So the exciting current range and the rotor position have to be considered for inductance computation. Except for no load machine study, the induced stator currents also have to be taken into account. As it deals with alternative currents, their amplitude and phasis besides the exciting field play an important role. To summarize, a stator phasis inductance L may be written:

$$L = f(\theta, I_\mathrm{e}, I, \Psi) \tag{3}$$

where θ is the rotor position, I_e, the exciting current amplitude, I the stator current amplitude (considering a balanced operating point), and Ψ its phasis besides the electromotive force. Accounting for all these parameters, many finite element computations are necessary to rightly characterise a salient pole saturated synchronous machine.

Expression (3) may be used for synchronous machine modeling in stator reference frame. However, to simplify the inductance computation, it is interesting to work in a synchronous rotating reference frame. By that way, two axis d and q are defined, d-axis is generally bounded to rotor saliency direction. In that frame, the previous expression (3) may be replaced by:

$$L_d = f_d(I_\mathrm{e}, I, \Psi), \qquad L_q = f_q(I_\mathrm{e}, I, \Psi). \tag{4}$$

Moreover, in most cases, accounting for the large air-gap, the induced currents do not act significantly; the inductances L_d and L_q may be simplified:

$$L_d = f_d(I_\mathrm{e}) \qquad L_q = cte. \tag{5}$$

These properties can be applied to synchronous machine modeling in a synchronous rotating reference frame, at least for steady state operating points; we don't speak of transient inductances due to damping bars which also have to be considered for dynamic operations.

Induction machine

As for the induction machine, the problem is rather different: leakage and magnetising inductances or again cyclic stator and rotor inductances may be introduced. On a general point of view, all these parameters are influenced by saturation effect. Principally, main inductances are depending on the instantaneous value of rotating magnetic field, besides, leakage parameters may also depend on the instantaneous values of stator and rotor currents. This last point is particularly sensitive for closed rotor slot machines [5]. For opened or half opened slot machine, we shall consider the influence of the resulting magnetic field on the value of the main inductances. Leakage inductances will be indirectly concerned by the computation, as they are included in the main parameters. Except the slotting effect, mechanical saliency effect does not occur in induction machine; however, accounting for our computation assumptions, we are expected to find a "magnetic saliency" due to saturation effect and following the rotating field instantaneous position around the air gap [6]. So the inductances will be computed according to two variables: the position and amplitude of the resulting magnetic field in the machine.

3 First approach: finite element computation

3.1 Three-phase/n-phase machine parameters

The first idea is to compute the parameters of the usual stator, rotor and mutual stator-rotor matrix respectively ($\mathcal{L}_\mathrm{s}$), ($\mathcal{L}_\mathrm{r}$) and ($\mathcal{M}_\mathrm{sr}$). First of all, for a squirrel cage rotor with n bars, it is necessary to define rotor phases. Several solutions exist; the most general way, independently of rotor bars number, is to consider one rotor phase constituted by two neighbouring bars, connected by two endring shares, building a mesh.

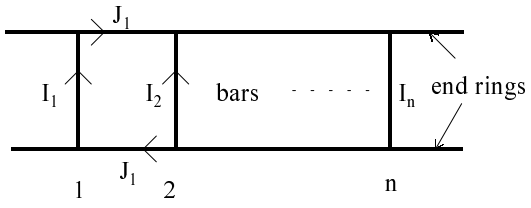

Fig. 2. Squirrel cage rotor phases representation.

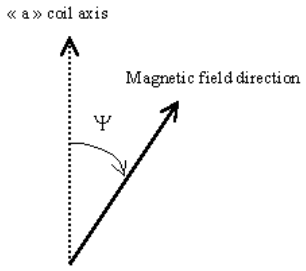

(a)

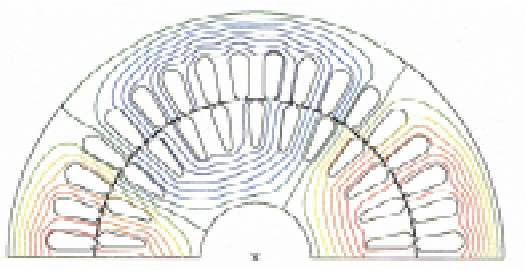

(b)

Fig. 3. (a) Field angle definition, (b) no load field distribution of the studied machine.

By that way, such rotor phases are effectively short-circuited. The phase current is the mesh current, that is the end-ring part current (Fig. 2).

Let us give the example of L_{aa} computation for a given range value of the rotating magnetic field and according to its position (L_{aa} is the self inductance of the a stator phase). The computation has two steps. In the first one, the corresponding magnetic state has to be enforced in the machine. We may apply three stator currents (magnetising current at no-load) or three rotor currents (n for a squirrel rotor cage with n bars) or both solutions. These approaches are almost similar as regards with the magnetic air gap field. However, they differ about the local magnetic state of each armature. Neglecting this phenomenon, it is easier to enforce stator three phase currents corresponding to rated magnetising current for instance. Then, each current value has to be chosen according to the desired position of the magnetic field. We shall note Ψ the electric field angle, referred, for instance, to the stator a-phase axis (Fig. 3a). This first computation gives the magnetic vector potential value at each node of the mesh, so the magnetic state is defined locally. The resulting permeability is kept for the second computation step. In order to calculate L_{aa}, and following its definition, it is necessary to compute ϕ_{aa}, the a-phase flux linkage when only the a stator phase current occurs. It is a linear finite element computation, with the permeability of the previous step. The flux computation is deduced from the magnetic vector potential knowledge as explained in Section 2.2.

This method may be repeated for different rotating field instantaneous positions, that is for different phase values of the stator currents during the first step. Then the computation may also be extended to different values of the amplitude of the magnetising current.

The approach is quite similar for the computation of the other coefficients of the stator inductance matrix. It may also be applied for the calculation of the $(\mathcal{M}_{\rm sr})$ and $(\mathcal{L}_{\rm r})$ matrix; as a remark, the $(\mathcal{M}_{\rm sr})$ matrix depends on the relative stator-rotor position θ. To avoid a great number of computations, we suppose that rotation and saturation effects are decoupling phenomena, which means that mutual inductances are considered sinusoidally θ depending. According to this assumption, the consideration of saturation effect is done for a given value of θ, in particular, θ equal to zero. The most important result of these computations is the particular waveform of the inductance coefficients as a function of Ψ, the magnetic rotating field angle [6]. Effectively, at least for regular geometry armatures, which involves that the saturation effect occurs in the same manner for all the coils, the computed coefficients vary sinusoidally with the angle 2Ψ. From these results, the influence of rotating field may be described as follow:

$$(\mathcal{L}_{\rm s}) = \begin{bmatrix} L_{\rm s} & -M_{\rm s} & M_{\rm s} \\ -M_{\rm s} & L_{\rm s} & M_{\rm s} \\ -M_{\rm s} & M_{\rm s} & L_{\rm s} \end{bmatrix} + \Delta L_{\rm s} \begin{bmatrix} \cos 2\Psi & \cos(2\Psi - 2\pi/3) & \cos(2\Psi + 2\pi/3) \\ \cos(2\Psi - 2\pi/3) & \cos(2\Psi + 2\pi/3) & \cos 2\Psi \\ \cos(2\Psi + 2\pi/3) & \cos 2\Psi & \cos(2\Psi - 2\pi/3) \end{bmatrix}. \quad (6)$$

As for $(\mathcal{L}_{\rm r})$ the rotor inductances matrix and $(\mathcal{M}_{\rm sr})$ the stator and rotor inductances matrix, they are also written following a similar expression and thanks to $\Delta L_{\rm r}$ and $\Delta M_{\rm sr}$ parameters. The values of $\Delta L_{\rm s}$, $\Delta L_{\rm r}$ and $\Delta M_{\rm sr}$ depend on the amplitude of the magnetic rotating field. In particular for an unsaturated operating point, their values are zero. On the other hand, they are all the more large that the saturation effect is important. For a given machine, they are also depending on the core geometry: in particular the ratio between the yoke length and the distance between two neighbouring slots enforce the sign of these coefficients [7]. This study deals with an induction machine whose geometry is portrayed in Figure 4. For that kind of motor, the saturated areas for a given position of rotating magnetic field are the teeth located in the field direction.

Consequently, for Ψ equal to zero, (the magnetic field is in the stator a-phasis direction), the "a" stator phase self inductance decreases because of saturation effect over the

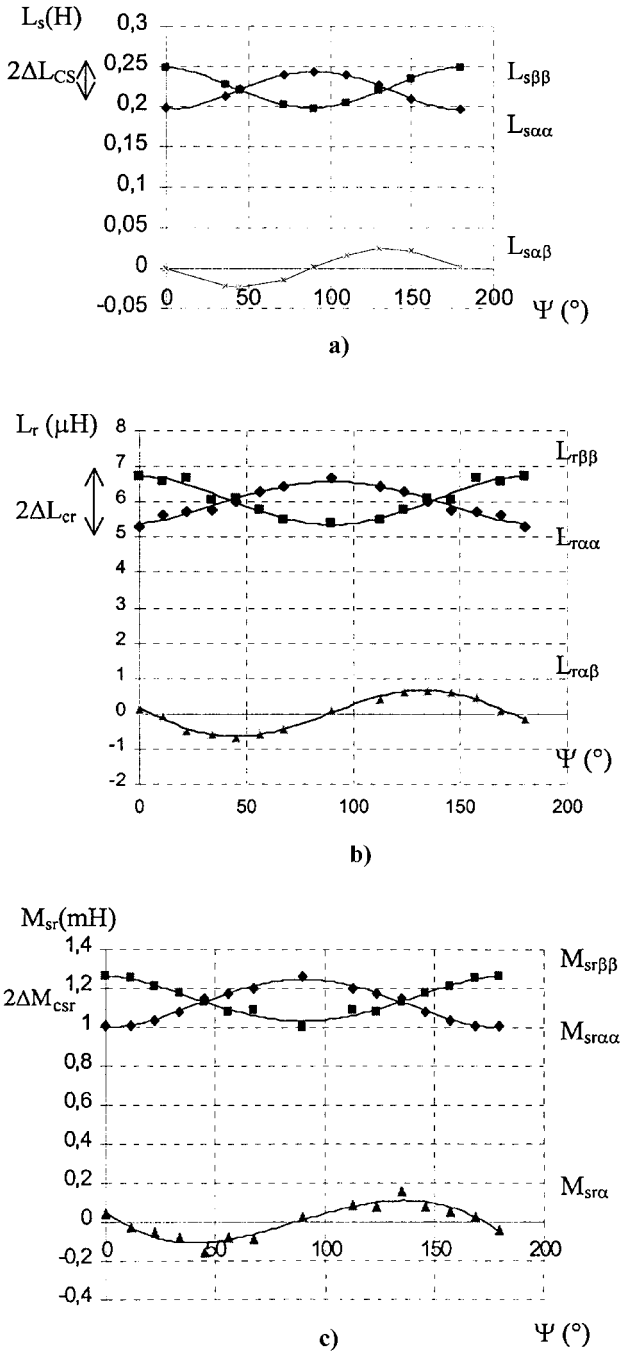

Fig. 4. Evolution of inductance matrix coefficients in a fixed reference frame as a function of magnetic field position (i_μ = 5.55 A): (a) stator inductances, (b) rotor inductances, (c) stator/rotor mutual inductances.

area used to compute its flux linkage. That also means a negative ΔL_s, following equation (6). On the other hand, when the yoke length is particularly thin, the most important saturation effect occurs in the yoke located with a space angle $\pi/2p$ besides the rotating field axis. Then, ΔL_s and the other similar coefficients are positive [7].

Besides, the balanced waveform of inductances, which means that saturation effect occurs with the same manner for the three phases, allows the computation of the equivalent two phase machine inductances.

3.2 Equivalent two phase induction machine

To compute inductive parameters of the two-phases equivalent machine, it is first necessary to define the new stator and rotor phase coils referred to the same reference fame. By that way, the dependency upon rotor position can be avoided. For that aim, the well-known three-two transformation T_{32} (Concordia) is used to describe stator coils. As for the rotor, accounting for the phase definition given in Section 3.1, a normalized n phases/two phases transformation is introduced to obtain the new two phase rotor coil:

$$T_{n2} = \sqrt{\frac{2p}{n}} \begin{bmatrix} 1 & 0 \\ \cos(2p\pi/n) & \sin(2p\pi/n) \\ \cos(4p\pi/n) & \sin(4p\pi/n) \\ \vdots & \vdots \\ \cos(2(n-1)p\pi/n) & \sin(2(n-1)p\pi/n) \end{bmatrix}. \tag{7}$$

Moreover, to simplify the mutual inductance computation, the rotor phases are defined so that the 1-phase axis coincides with the a stator phase, and the rotation matrix $P(-p\theta)$ is applied to rotor windings

$$P(p\theta) = \begin{pmatrix} \cos p\theta & -\sin p\theta \\ \sin p\theta & \cos p\theta \end{pmatrix}. \tag{8}$$

From the two phase machine modeling, new inductance matrix are introduced for both armatures:

$$(L_\mathrm{s}) = \begin{pmatrix} L_{\mathrm{s}\alpha\alpha} & L_{\mathrm{s}\alpha\beta} \\ L_{\mathrm{s}\beta\alpha} & L_{\mathrm{s}\beta\beta} \end{pmatrix},$$

$$(L_\mathrm{r}) = \begin{pmatrix} L_{\mathrm{r}\alpha\alpha} & L_{\mathrm{r}\alpha\beta} \\ L_{\mathrm{r}\beta\alpha} & L_{\mathrm{r}\beta\beta} \end{pmatrix},$$

$$\text{and} \quad (M_\mathrm{sr}) = \begin{pmatrix} M_{\mathrm{sr}\alpha\alpha} & M_{\mathrm{sr}\alpha\beta} \\ M_{\mathrm{sr}\beta\alpha} & M_{\mathrm{sr}\beta\beta} \end{pmatrix}. \tag{9}$$

To compute all these new coefficients, we have to work with the two-phase machine fluxes and currents:

$$\begin{pmatrix} \phi_\alpha \\ \phi_\beta \end{pmatrix}_\mathrm{s} = T_{32}^t \begin{pmatrix} \phi_a \\ \phi_b \\ \phi_c \end{pmatrix}; \quad \begin{pmatrix} \phi_\alpha \\ \phi_\beta \end{pmatrix}_\mathrm{r} = T_{n2}^t \begin{pmatrix} \phi_1 \\ \vdots \\ \phi_n \end{pmatrix};$$

$$\begin{pmatrix} I_\alpha \\ I_\beta \end{pmatrix}_\mathrm{s} = T_{32}^t \begin{pmatrix} i_a \\ i_b \\ i_c \end{pmatrix}; \quad \begin{pmatrix} J_\alpha \\ J_\beta \end{pmatrix}_\mathrm{r} = T_{n2}^t \begin{pmatrix} J_1 \\ \vdots \\ J_n \end{pmatrix}. \tag{10}$$

It may be noted that the J_i currents correspond to end-ring currents. However, for a 2D finite element computation, only bars currents are able to be enforced. So it is necessary to express bars currents as a function of rotor phase ones.

4 Computation results

The computed results are obtained for the squirrel-cage machine described in appendix, at the end of the paper. Two sets of results are given, respectively for the rated magnetising current (maximum value, 5.55 A) and for i_μ equal to 10 A.

Figure 4 portrays the waveforms of each inductance coefficient for the rated value of magnetising current, and following the instantaneous field position angle. As expected from the three-phase-machine results, the obtained curves are quasi-sinusoidal [6]; moreover, the variation range is quite similar for the parameters belonging to the same inductance matrix. In Figure 4, a few discrepancies appear between computed points and sinusoidal interpolation: they may be partly explained by the slotting effect, which locally modifies the corresponding phase permeance.

Another set of computed results have been obtained for a higher value of magnetising current: Figure 5 shows the inductance coefficients behaviour for $i_\mu = 10$ A.

From these particular waveforms, the inductance matrix may be expressed as:

$$(L_\mathrm{s}) = \begin{pmatrix} L_\mathrm{ms} & 0 \\ 0 & L_\mathrm{ms} \end{pmatrix} + \Delta L_\mathrm{cs}\, R(\Psi),$$

$$(L_\mathrm{r}) = \begin{pmatrix} L_\mathrm{mr} & 0 \\ 0 & L_\mathrm{mr} \end{pmatrix} + \Delta L_\mathrm{cr}\, R(\Psi),$$

$$(M_\mathrm{sr}) = \begin{pmatrix} M_\mathrm{msr} & 0 \\ 0 & M_\mathrm{msr} \end{pmatrix} + \Delta M_\mathrm{csr}\, R(\Psi). \qquad (11)$$

L_ms, L_mr and M_msr represent the mean values of the different inductances and the Δ terms describe their amplitude variation (Figs. 4 and 5). $R(\Psi)$ has the following expression:

$$R(\Psi) = \begin{pmatrix} \cos 2\Psi & +\sin 2\Psi \\ +\sin 2\Psi & -\cos 2\Psi \end{pmatrix}. \qquad (12)$$

This matrix can also be written thanks to rotation matrix P:

$$R(\Psi) = P(\Psi) \begin{pmatrix} 1 & 0 \\ 0 & -1 \end{pmatrix} P(\Psi). \qquad (13)$$

Rotor and stator flux linkages are deduced from these expressions:

$$\begin{pmatrix} \phi_\alpha \\ \phi_\beta \end{pmatrix}_\mathrm{s} = L_\mathrm{ms} \begin{pmatrix} I_\alpha \\ I_\beta \end{pmatrix}_\mathrm{s} + M_\mathrm{msr} \begin{pmatrix} I_\alpha \\ I_\beta \end{pmatrix}_\mathrm{r} + P(\Psi) \begin{pmatrix} 1 & 0 \\ 0 & -1 \end{pmatrix} \times P(-\Psi) \left[\Delta L_\mathrm{cs} \begin{pmatrix} I_\alpha \\ I_\beta \end{pmatrix}_\mathrm{s} + \Delta M_\mathrm{csr} \begin{pmatrix} I_\alpha \\ I_\beta \end{pmatrix}_\mathrm{r} \right],$$

$$\begin{pmatrix} \phi_\alpha \\ \phi_\beta \end{pmatrix}_\mathrm{r} = L_\mathrm{mr} \begin{pmatrix} I_\alpha \\ I_\beta \end{pmatrix}_\mathrm{r} + M_\mathrm{msr} \begin{pmatrix} I_\alpha \\ I_\beta \end{pmatrix}_\mathrm{s} + P(\Psi) \begin{pmatrix} 1 & 0 \\ 0 & -1 \end{pmatrix} \times P(-\Psi) \left[\Delta L_\mathrm{cr} \begin{pmatrix} I_\alpha \\ I_\beta \end{pmatrix}_\mathrm{r} + \Delta M_\mathrm{csr} \begin{pmatrix} I_\alpha \\ I_\beta \end{pmatrix}_\mathrm{s} \right]. \qquad (14)$$

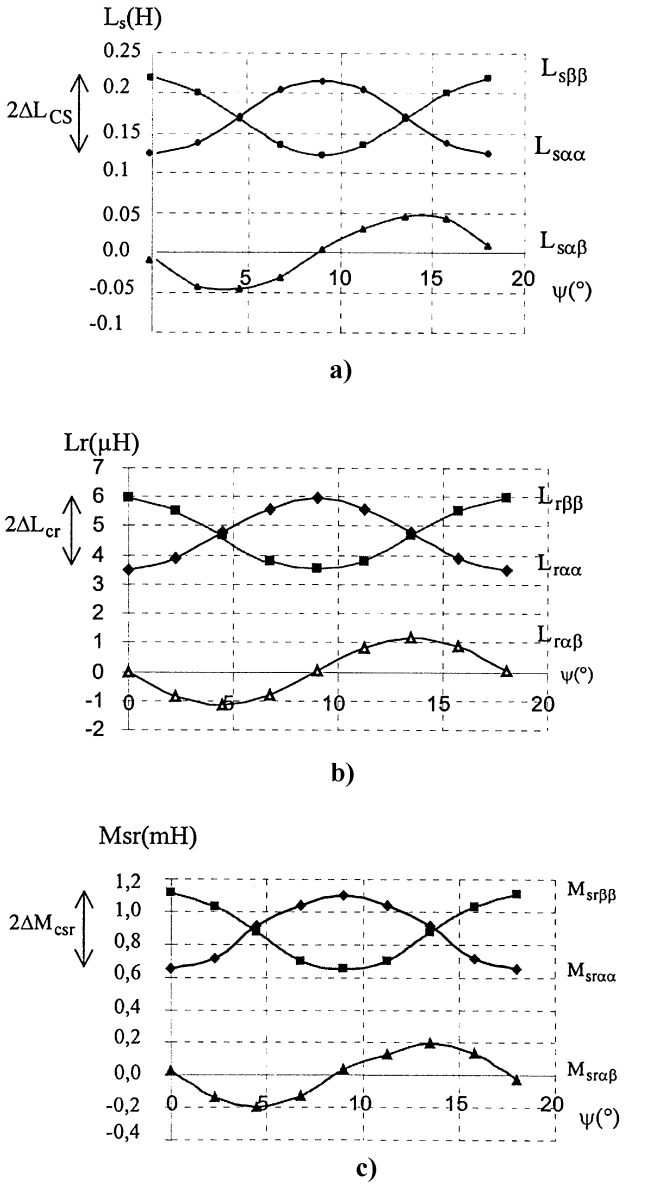

Fig. 5. Evolution of inductance matrix coefficients in a fixed reference frame as a function of magnetic field position, (i_μ = 10 A): (a) stator inductances, (b) rotor inductances, (c) stator/rotor mutual inductances.

The flux expression seems to be rather complicated. However, thanks to analytical theory, it is possible to express the fluxes in a simple way, with parameters accounting for saturation as we shall see in Section 6.

5 Second approach: extension of Park's modeling

The usual analytical approach deals with constant value inductance coefficients. We are going to extend its application range by considering saturated permeance. First, let us remind of the magnetomotive forces (*mmf*) and magnetising current expressions.

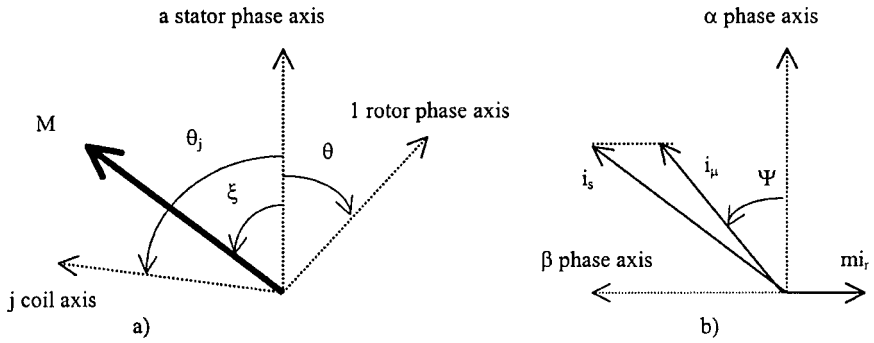

Fig. 6. Angle definition.

5.1 Magnetomotive forces and magnetising current

Following the first space harmonic assumption, the *mmf* are defined for one air-gap point denoted M, characterised by its position angle ξ besides a stator phase axis (Fig. 5a). As an example, ε_j, the *mmf* created by i_j the j stator phase current is written:

$$\varepsilon_j = A_\mathrm{s} i_j \cos p(\xi - \theta_j) \quad \text{with} \quad A_\mathrm{s} = \frac{2}{\pi} k_\mathrm{s} n_\mathrm{s}. \tag{15}$$

k_s and n_s are respectively the first harmonic winding coefficient and the turn number for one phase and one pole pair; θ_j is the mechanical angle which locates the j coil axis (Fig. 6a).

And for the rotor armature, the *mmf* of the k rotor phase is expressed as:

$$\varepsilon_k = A_\mathrm{r} i_k \cos p(\xi - \theta - \theta_k) \quad \text{with} \quad A_\mathrm{r} = \frac{2}{\pi} k_\mathrm{r} n_\mathrm{r}. \tag{16}$$

To simplify the expressions of the stator and rotor resulting *mmf* ε_s and ε_r, it is interesting to work in a fixed two-phase reference frame. Then the *mmf* amplitudes are respectively:

$$\varepsilon_\mathrm{sm}(t) = \sqrt{\frac{2}{3}} A_\mathrm{s} i_\mathrm{s}(t) \quad \text{and} \quad \varepsilon_\mathrm{rm}(t) = \sqrt{\frac{n}{2p}} A_\mathrm{r} i_\mathrm{r}(t). \tag{17}$$

Usually, the magnetising current is introduced as a stator current which would induce the same *mmf* as the total one ε_tm created by both stator and rotor currents. Let us note $i_\mu(t)$ the instantaneous value of magnetising current range (Fig. 6b). Following (17), the magnetising current has to verify:

$$\varepsilon_\mathrm{tm} = \sqrt{\frac{3}{2}} A_\mathrm{s} i_\mu(t). \tag{18}$$

From equations (17, 18), the stator/rotor transformation coefficient appears:

$$m = \frac{A_\mathrm{r}}{A_\mathrm{s}} \sqrt{\frac{n}{2p}} \sqrt{\frac{2}{3}}\,. \tag{19}$$

Finally, the two-phase magnetising current may be expressed as:

$$\begin{pmatrix} i_{\mu\alpha} \\ i_{\mu\beta} \end{pmatrix} = \begin{pmatrix} i_\alpha \\ i_\beta \end{pmatrix}_\mathrm{s} + m \begin{pmatrix} i_\alpha \\ i_\beta \end{pmatrix}_\mathrm{r}. \tag{20}$$

5.2 Equivalent saturated permeance: use of an equivalent magnetic saliency hypothesis

To take into account the saturation effect whose consequences on inductance values have been previously described, we may introduce a saturated permeance, depending on magnetising current vector instantaneous position. Effectively, it is possible to define an air gap permeance which would be smaller in the saturated area (in magnetising current axis for the machine example of Fig. 3, in the quadrature direction for the other eventuality).

From the previous finite element results which show quasi-sinusoidal variations of inductances, the saturated permeance expression may be limited to the second harmonic:

$$P = P_0(i_\mu) + P_2(i_\mu) \cos 2(p\xi - \Psi). \tag{21}$$

Besides, even if P corresponds to an air-gap permeance, its amplitude value still depends on magnetising current. Once again, for the kind of machine studied (Fig. 3), $P_2(i_\mu)$ is negative. *This permeance expression is quite similar to salient pole synchronous machine permeance, and characterises a magnetic saliency.* For low value of i_μ, the saliency term P_2 becomes null and P reaches the usual value μ_0/e, where e represents the air-gap length.

5.3 Analytical expression of saturated equivalent inductances

General expression

From the *mmf* and the air gap permeance previously introduced, it is possible to write the expression of B, the magnetic field induced on one air-gap point (M, ξ) by a current fed winding γ:

$$B = P\varepsilon_\gamma \quad \text{with} \quad \varepsilon_\gamma = A_\gamma i_\gamma \cos p(\xi - \gamma). \tag{22}$$

ε_γ is the *mmf* created by an exciting current i_γ flowing through a winding whose axis is located by the angle γ.

Let us now consider another winding, characterised by its angle δ, the flux ϕ_δ induced by the *mmf* ε_γ is expressed:

$$\phi_\delta = p\mathcal{I} \int_{\delta - \frac{\pi}{2p}}^{\delta + \frac{\pi}{2p}} k_\delta n_\delta B \frac{D}{2} \mathrm{d}\xi \tag{23}$$

$$\begin{pmatrix}\phi_\alpha\\ \phi_\beta\end{pmatrix}_{\rm s} = \left[\ell_1 I_{2\times2} + \frac{3}{2}L_{\rm s0}I_{2\times2} + \frac{3}{2}L_{\rm s2}P(\Psi)\begin{bmatrix}1&0\\0&-1\end{bmatrix}P(-\Psi)\right]\begin{pmatrix}i_\alpha\\ i_\beta\end{pmatrix}_{\rm s} + \left[\sqrt{\frac{3}{2}}\sqrt{\frac{n}{2p}}L_{\rm sr0}I_{2\times2} + \sqrt{\frac{3}{2}}\sqrt{\frac{n}{2p}}L_{\rm sr2}P(\Psi)\begin{bmatrix}1&0\\0&-1\end{bmatrix}P(-\Psi)\right]\begin{pmatrix}i_\alpha\\ i_\beta\end{pmatrix}_{\rm r} \quad (31)$$

and

$$\begin{pmatrix}\phi_\alpha\\ \phi_\beta\end{pmatrix}_{\rm r} = \left[\ell_2 I_{2\times2} + \frac{n}{2p}L_{\rm r0}I_{2\times2} + \frac{n}{2p}L_{\rm r2}P(\Psi)\begin{bmatrix}1&0\\0&-1\end{bmatrix}P(\Psi)\right]\begin{pmatrix}i_\alpha\\ i_\beta\end{pmatrix}_{\rm r} + \left[\sqrt{\frac{n}{2p}}\sqrt{\frac{3}{2}}L_{\rm sr0}I_{2\times2} + \sqrt{\frac{n}{2p}}\sqrt{\frac{3}{2}}L_{\rm sr2}P(\Psi)\begin{bmatrix}1&0\\0&-1\end{bmatrix}P(\Psi)\right]\begin{pmatrix}i_\alpha\\ i_\beta\end{pmatrix}_{\rm s} \quad (32)$$

with D the air-gap diameter and $\mathcal{I}$ the machine length. According to equations (21, 22, 23), the flux ϕ_δ may also be written following the first space harmonic:

$$\phi_\delta = [L_{\delta\gamma0}\cos p(\delta-\gamma) + L_{\delta\gamma2}\cos(p\delta+p\gamma-2\Psi)]i_\gamma. \quad (24)$$

Two inductive coefficients appear in (24):

$$L_{\delta\gamma0} = \frac{\mathcal{I}D}{\pi}(k_\delta n_\delta)(k_\gamma n_\gamma)2P_0(i_\mu) \quad (25)$$

and

$$L_{\delta\gamma2} = \frac{\mathcal{I}D}{\pi}(k_\delta n_\delta)(k_\gamma n_\gamma)P_2(i_\mu). \quad (26)$$

It may be remarked that the classical analytical approach only considers the term $L_{\delta\gamma0}$ with $P_0 = \mu_0/e$.

Induction machine inductance expression

Let us now apply the formulations (25, 26) to a three-phase stator windings of an induction machine. In that case, the stator inductance matrix may be written in two parts:

$$(\mathcal{L}_{\rm s}) = (\mathcal{L}_{\rm s0}) + (\mathcal{L}_{\rm s2}(\Psi)) \quad (27)$$

$$\text{with } (\mathcal{L}_{\rm s0}) = \begin{pmatrix}L_{\rm s0}&M_{\rm s0}&M_{\rm s0}\\M_{\rm s0}&L_{\rm s0}&M_{\rm s0}\\M_{\rm s0}&M_{\rm s0}&L_{\rm s0}\end{pmatrix}$$

$$\text{and } (\mathcal{L}_{\rm s2}) = L_{\rm s2}\begin{pmatrix}\cos2\Psi & \cos(2\Psi-2\pi/3) & \cos(2\Psi+2\pi/3)\\ \cos(2\Psi-2\pi/3) & \cos(2\Psi+2\pi/3) & \cos2\Psi\\ \cos(2\Psi+2\pi/3) & \cos2\Psi & \cos(2\Psi-2\pi/3)\end{pmatrix}. \quad (28)$$

$L_{\rm s0}$, $L_{\rm s2}$ and $M_{\rm s0}$ are written in the particular case of a balanced induction machine with the first space harmonic assumption:

$$L_{\rm s0} = \frac{\mathcal{I}D}{\pi}(k_{\rm s}n_{\rm s})^2 2P_0,$$
$$M_{\rm s0} = -\frac{1}{2}L_{\rm s0},$$
$$L_{\rm s2} = \frac{\mathcal{I}D}{\pi}(k_{\rm s}n_{\rm s})^2 P_2. \quad (29)$$

At this stage, to compare the expressions (28, 6), it may be noted that the classical analytical approach does not take into account leakage fluxes. To consider this phenomenon, a new leakage matrix $[\mathcal{I}_{\rm s}]$ must be added to the right term of (27).

The factorization properties of $[\mathcal{L}_{\rm s0}]$ and $[\mathcal{I}_{\rm s}]$ are well-known. To simplify the characterisation of the equivalent two phase machine, we may remark that $[\mathcal{L}_{\rm s2}]$ can also be expressed as following:

$$[\mathcal{L}_{\rm s2}] = \frac{3}{2}L_{\rm s2}T_{32}R(\Psi)T_{32}^t. \quad (30)$$

As for the rotor inductance and stator/rotor mutual inductance matrix, their expressions are quite similar; $L_{\rm r0}$, $M_{\rm r0}$, and $L_{\rm r2}$ may be defined as previously, replacing $k_{\rm s}$ and $n_{\rm s}$ by $k_{\rm r}$ and $n_{\rm r}$ in (29). A leakage inductance matrix $[\mathcal{I}_{\rm r}]$ as well as main inductance matrix $[\mathcal{L}_{\rm r0}]$ and $[\mathcal{L}_{\rm r2}]$ may be also introduced. Their factorizations need the T_{n2} transformation and a coefficient $n/2p$ appears. In a similar way, $L_{\rm sr0}$, $M_{\rm sr0}$ and $L_{\rm sr2}$ are written, replacing the term $(k_{\rm s}n_{\rm s})^2$ in (29) by the product $(k_{\rm s}n_{\rm s})(k_{\rm r}n_{\rm r})$; after factorization, the matrix $[\mathcal{M}_{\rm sr0}]$ and $[\mathcal{M}_{\rm sr2}]$ are written with a coefficient $\sqrt{3/2}\sqrt{n/2p}$.

We shall not give more details about this three-phase/n-phase machine modeling; accounting for the transformation properties of the inductance matrix, it is much more interesting to study the equivalent two phase machine.

Equivalent two phases machine flux expression

From the two transformations previously introduced, and thanks to the rotation matrix $P(p\theta)$, the fluxes of the equivalent two phase machine referred to a fixe reference frame can be written:

see equations (31, 32) above.

The coefficients ℓ_1 and ℓ_2 which appear in the previous equations correspond to cyclic leakage stator and rotor inductances.

These expressions may be compared with equations (14) obtained from finite element computation. From

this comparison, the different coefficients may be identified: so for the stator, we obtain theoretically:

$$L_{\mathrm{ms}} = \ell_1 + \frac{3}{2}L_{\mathrm{s0}} \quad \text{and} \quad \Delta L_{\mathrm{cs}} = \frac{3}{2}L_{\mathrm{s2}}. \tag{33}$$

For the rotor armature:

$$L_{\mathrm{mr}} = \ell_2 + \frac{n}{2p}L_{\mathrm{r0}} \quad \text{and} \quad \Delta L_{\mathrm{cr}} = \frac{n}{2p}L_{\mathrm{r2}}. \tag{34}$$

As for the stator/rotor mutual inductance coefficients:

$$M_{\mathrm{msr}} = \sqrt{\frac{3}{2}}\sqrt{\frac{n}{2p}}L_{\mathrm{sr0}} \quad \text{and} \quad \Delta M_{\mathrm{csr}} = \sqrt{\frac{3}{2}}\sqrt{\frac{n}{2p}}L_{\mathrm{sr2}}. \tag{35}$$

Of course, writing these equalities involves particular relations between the coefficients computed from FEM. Effectively, from the analytical approach, these parameters are bounded by the transformation ratio m introduced in equation (19).

Analytical approach check-up

The analytical approach previously developed works with the assumption of a second permeance harmonic P_2, which implies relationships between the different inductances introduced. In particular, from equations (33, 34, 35), it appears that the variation coefficients provided by the analytical approach are bounded by the following relation (36):

$$\frac{\Delta L_{\mathrm{cs}}}{\Delta M_{\mathrm{csr}}} = \frac{\Delta M_{\mathrm{csr}}}{\Delta L_{\mathrm{cr}}} = \sqrt{\left(\frac{\Delta L_{\mathrm{cs}}}{\Delta L_{\mathrm{cr}}}\right)} = \frac{1}{m}\,. \tag{36}$$

Let us check this assumption with the FEM computation results. Table 1 summarizes and compares the results obtained from the two finite element computations, as well as the theoretical value of the transformation ratio m, calculated from the winding data of the machine (see Appendix).

These results are quite satisfactory accounting for the accuracy of the finite element computations and although the assumptions we have done using the analytical method (first space harmonic, constant value for leakage inductances, ...). The good agreement between the finite element computations allows to check the second harmonic permeance assumption, and give a way to compute the transformation ratio m. It may be reminded that the calculation of this transformation ratio from the mains terms $(L_{\mathrm{s}}, M_{\mathrm{sr}}, L_{\mathrm{r}})$, neglecting the leakage inductances, would give inaccurate results.

6 Synthesis of the results

6.1 Simplification of flux expressions

The flux equations written in the previous part, seem to be quite complicated and difficult to use for simulation. Moreover they depend on Ψ angle, the phase of magnetising current which does not appear specifically in (14). So let us introduce the magnetising current i_μ thanks to its definition given in (20).

Accounting for the coefficients L_{r0}, L_{r2} and the transformation ratio m, it is possible to write:

$$\begin{aligned}\begin{pmatrix}\phi_\alpha\\ \phi_\beta\end{pmatrix}_{\mathrm{s}} &= \ell_1 \begin{pmatrix}i_\alpha\\ i_\beta\end{pmatrix}_{\mathrm{s}} + \frac{3}{2}L_{\mathrm{s0}}\begin{pmatrix}i_{\mu\alpha}\\ i_{\mu\beta}\end{pmatrix},\\ &\quad + \frac{3}{2}L_{\mathrm{s2}}P(\Psi)\begin{bmatrix}1 & 0\\ 0 & -1\end{bmatrix}P(-\Psi)\begin{pmatrix}i_{\mu\alpha}\\ i_{\mu\beta}\end{pmatrix},\end{aligned} \tag{37}$$

$$\begin{aligned}\begin{pmatrix}\phi_\alpha\\ \phi_\beta\end{pmatrix}_{\mathrm{r}} &= \ell_1 \begin{pmatrix}i_\alpha\\ i_\beta\end{pmatrix}_{\mathrm{r}} + \frac{n}{2p}\frac{L_{\mathrm{r0}}}{m}\begin{pmatrix}i_{\mu\alpha}\\ i_{\mu\beta}\end{pmatrix}\\ &\quad + \frac{n}{2p}\frac{L_{\mathrm{r2}}}{m}P(\Psi)\begin{bmatrix}1 & 0\\ 0 & -1\end{bmatrix}P(-\Psi)\begin{pmatrix}i_{\mu\alpha}\\ i_{\mu\beta}\end{pmatrix}.\end{aligned} \tag{38}$$

To simplify these equations, it may be remarked that, referred to the stator reference frame, the magnetising current is written as:

$$\begin{pmatrix}i_{\mu\alpha}\\ i_{\mu\beta}\end{pmatrix} = i_\mu P(\Psi)\begin{bmatrix}1\\ 0\end{bmatrix}. \tag{39}$$

So flux expressions are reduced to:

$$\begin{pmatrix}\phi_\alpha\\ \phi_\beta\end{pmatrix}_{\mathrm{s}} = \ell_1 \begin{pmatrix}i_\alpha\\ i_\beta\end{pmatrix}_{\mathrm{s}} + \left(\frac{3}{2}L_{\mathrm{s0}} + \frac{3}{2}L_{\mathrm{s2}}\right)\begin{pmatrix}i_{\mu\alpha}\\ i_{\mu\beta}\end{pmatrix} \tag{40}$$

and

$$\begin{pmatrix}\phi_\alpha\\ \phi_\beta\end{pmatrix}_{\mathrm{r}} = \ell_2 \begin{pmatrix}i_\alpha\\ i_\beta\end{pmatrix}_{\mathrm{r}} + \left(\frac{n}{2p}L_{\mathrm{r0}} + \frac{n}{2p}L_{\mathrm{r2}}\right)\frac{1}{m}\begin{pmatrix}i_{\mu\alpha}\\ i_{\mu\beta}\end{pmatrix}. \tag{41}$$

Replacing the magnetising current by its expression (20) stator and rotor fluxes of the two phase machine may also be expressed as a straightforward function of stator and rotor currents [8]:

$$\begin{aligned}\begin{pmatrix}\phi_\alpha\\ \phi_\beta\end{pmatrix}_{\mathrm{s}} &= \left(\ell_1 + \frac{3}{2}L_{\mathrm{s0}} + \frac{3}{2}L_{\mathrm{s2}}\right)\begin{pmatrix}i_\alpha\\ i_\beta\end{pmatrix}_{\mathrm{s}}\\ &\quad + \sqrt{\frac{3}{2}}\sqrt{\frac{n}{2p}}(L_{\mathrm{sr0}} + L_{\mathrm{sr2}})\begin{pmatrix}i_\alpha\\ i_\beta\end{pmatrix}_{\mathrm{r}}\end{aligned} \tag{42}$$

and

$$\begin{aligned}\begin{pmatrix}\phi_\alpha\\ \phi_\beta\end{pmatrix}_{\mathrm{r}} &= \left(\ell_2 + \frac{n}{2p}L_{\mathrm{r0}} + \frac{n}{2p}L_{\mathrm{r2}}\right)\begin{pmatrix}i_\alpha\\ i_\beta\end{pmatrix}_{\mathrm{r}}\\ &\quad + \sqrt{\frac{3}{2}}\sqrt{\frac{n}{2p}}(L_{\mathrm{sr0}} + L_{\mathrm{sr2}})\begin{pmatrix}i_\alpha\\ i_\beta\end{pmatrix}_{\mathrm{s}}.\end{aligned} \tag{43}$$

These results are quite similar to classical analytical approach results; they allow to introduce the usual cyclic inductances $\mathcal{L}_{\mathrm{cs}}$ (stator), $\mathcal{L}_{\mathrm{cr}}$ (rotor), $\mathcal{M}_{\mathrm{sr}}$ (stator/rotor) such that:

$$\begin{aligned}\mathcal{L}_{\mathrm{cs}} &= \ell_1 + \frac{3}{2}(L_{\mathrm{s0}} + L_{\mathrm{s2}}),\\ \mathcal{L}_{\mathrm{cr}} &= \ell_2 + \frac{n}{2p}(L_{\mathrm{r0}} + L_{\mathrm{r2}}),\\ \mathcal{M}_{\mathrm{sr}} &= \sqrt{\frac{3}{2}}\sqrt{\frac{n}{2p}}(L_{\mathrm{sr0}} + L_{\mathrm{sr2}}).\end{aligned} \tag{44}$$

Table 1. Comparison between FEM and analytical approach results.

FEM					Analytical approach
$I_\mu(A)$	$\Delta L_{cs}/\Delta M_{csr}$ $(1/m_1)$	$\Delta M_{csr}/\Delta L_{cr}$ $(1/m_2)$	$\sqrt{\Delta L_{cs}/\Delta L_{cr}}$ $(1/m_3)$	Mean value of $1/m_1$, $1/m_2$, $1/m_3$	$1/m$
5.55	183.8	188.4	186.1	186.1	182.3
10	196	188	196	193.3	
		Error (%) besides the two FEM computations		3.8%	

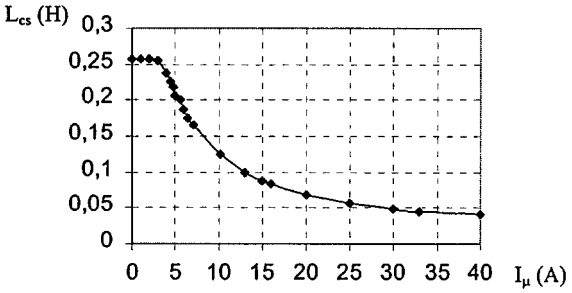

Fig. 7. Stator cyclic inductance evolution besides magnetising current value.

6.2 Extended Park model

From the previous flux expressions, we can deduce that the magnetising current angle Ψ has no influence on the two phase machine flux [8,9]. Besides, we could have deduced the same conclusion for the three phase machine; on the contrary, all the cyclic inductance values depend on magnetising current level.

Computation methodology

Even if the results do not seem to be new besides usual analytical approach, they involve a methodology of inductance computation: for a given range value of magnetising current, only one finite element computation is necessary to determine the values of $\mathcal{L}_{cs}$, $\mathcal{M}_{sr}$ and $\mathcal{L}_{cr}$. Accounting for (44), the coefficients useful for flux expression can be obtain for a null value of Ψ. For that aim, the magnetising current vector must be enforced following the axis of the equivalent two-phase winding whose coefficient is calculated. As for the two computation steps described in Section 3.1, they may be replaced by a single one.

Of course, these calculations must be repeated for each magnetising current range value. For instance, Figure 7 portrays the evolution of $\mathcal{L}_{cs}$ as a function of i_μ.

Determination of leakage parameters

The analytical approach works with constant leakage inductance assumption. FEM do not make any assumption about this point, as it computes cyclic inductances behaviour, including leakage coefficient. The low variations of the transformation ratio m as a function of the magnetising current (Tab. 1) gives an idea about the leakage inductances variations. In our case (semi-opened slots machine) they may not vary considerably [14]. Nevertheless, it is rather difficult to determine these coefficients analytically. Several methods exist to compute their values and their variations from FEM [10,11]. With our approach, thanks to the transformation ratio calculation, it is possible to determine ℓ_1 and ℓ_2:

$$\ell_1 = \mathcal{L}_{cs} - \frac{\mathcal{M}_{sr}}{m}, \quad \ell_2 = \mathcal{L}_{cr} - m\mathcal{M}_{sr}. \tag{45}$$

As an example, the numerical values of leakage inductances for the studied machine and for the rated magnetising current are respectively 16.3 mH for ℓ_1 and 0.143 mH for ℓ_2, this value being already referred to the stator armature thanks to "m" coefficient. However, it may be noted that this leakage inductance computation is very sensitive with the inaccuracy of the coefficients which appear in equation (45).

State equations

To study the voltage fed induction machine, it is necessary to write state equations, and to choose state variables.

Effectively, the usual choice is to consider stator and rotor currents, or stator and magnetising currents, as state variables. In that case, accounting to the parameter variations with the magnetising current, dynamic inductances appear in state equations [12]. On the other hand, to simplify the computation, it is interesting to work with stator and rotor fluxes as state variables [9]. Then the state matrix is unchanged for linear or saturated cases, only the coefficient values vary with saturation effect

$$\frac{\mathrm{d}}{\mathrm{d}t}\begin{pmatrix}\phi_{\alpha s}\\ \phi_{\beta s}\\ \phi_{\alpha r}\\ \phi_{\alpha r}\end{pmatrix} = \begin{pmatrix} -\frac{R_s}{\sigma\mathcal{L}_{cs}} & 0 & \frac{R_s\mathcal{M}_{sr}}{\sigma\mathcal{L}_{cs}\mathcal{L}_{cr}} & 0 \\ 0 & -\frac{R_s}{\sigma\mathcal{L}_{cs}} & 0 & \frac{R_s\mathcal{M}_{sr}}{\sigma\mathcal{L}_{cs}\mathcal{L}_{cr}} \\ \frac{R_r\mathcal{M}_{sr}}{\sigma\mathcal{L}_{cs}\mathcal{L}_{cr}} & 0 & -\frac{R_r}{\sigma\mathcal{L}_{cr}} & -p\Omega \\ 0 & \frac{R_r\mathcal{M}_{sr}}{\sigma\mathcal{L}_{cs}\mathcal{L}_{cr}} & p\Omega & -\frac{R_r}{\sigma\mathcal{L}_{cr}} \end{pmatrix}\begin{pmatrix}\phi_{\alpha s}\\ \phi_{\beta s}\\ \phi_{\alpha r}\\ \phi_{\alpha r}\end{pmatrix} + \begin{pmatrix}1&0\\0&1\\0&0\\0&0\end{pmatrix}\begin{pmatrix}v_{\alpha s}\\ v_{\beta s}\end{pmatrix}. \tag{46}$$

σ is the dispersion coefficient, R_s and R_r are respectively the stator phase and rotor phase resistances, and Ω, the

rotation speed. The fluxes are expressed in a fixed reference frame. To solve this state equation, the Euler method can be used; as the inductance parameters depend on magnetising current i_μ, it has to be computed at each time step from the flux values:

$$\begin{pmatrix} i_{\mu\alpha} \\ i_{\mu\beta} \end{pmatrix} = \left(\frac{1}{\sigma L_{\rm cs}} - \frac{M_{\rm sr}}{\sigma L_{\rm cs} L_{\rm cr}} \right) \begin{pmatrix} \phi_{\alpha{\rm s}} \\ \phi_{\beta{\rm s}} \end{pmatrix} + \left(\frac{1}{\sigma L_{\rm cs}} - \frac{M_{\rm sr}}{\sigma L_{\rm cs} L_{\rm cr}} \right) \begin{pmatrix} \phi_{\alpha{\rm r}} \\ \phi_{\beta{\rm r}} \end{pmatrix}. \quad (47)$$

Then, the new inductance values can be deduced from finite element computed characteristics and an iterative method is necessary to solve the non linear equations

Study of the modeling accuracy

In order to check the accuracy of the method previously developed, we have study two operating points of our machine: at no load and for nominal load. The extended analytical approach results are compared with those obtained from a FEM computation which considers the voltage supply, the shaft rotation and the saturation effect.

First, the machine is studied at no load, for nominal voltage supply (220 V per phase, 1500 rpm).

The use of linear assumption to compute stator currents with the analytical approach or with FEM gives very closed results. The current waveforms are sinusoidal and we can note a discrepancy less than 5% between the maximum values given by the both methods: $I_{\rm smax} = 3.68$ A by analytical approach, $I_{\rm smax} = 3.53$ A by FEM. Then the saturation effect is well taken into account, following the approach developed before for analytical method, thanks to an interpolation of B(H) curve and Newton-Raphson iterative procedure for FEM. In a first time, as the analytical approach does not consider any slotting effect, to compare with FEM results, the rotor bar conductivity has been enforced to zero value for finite element computation. The results are shown in Figure 7. Once again, the results are quite closed; besides linear case, we can note the rise due to saturation effect, and a difference of about 5% between the two method results.

In a second time, to show the slotting effect influence, the previous finite element computation results are compared with those obtained with the bar conductivity consideration. We can remark the effect of magnetic saturation which distorts the current waveforms for the last FEM results (Fig. 8). This behaviour may be explained by the space harmonics. Effectively, classical 6th harmonics are induced in rotor bars due to winding distribution and slotting effect; at no load, these bar currents create 5th harmonic in stator coils, which seems to be increased when saturation occurs.

Nevertheless, despite this discrepancy about the waveform, the extended analytical and finite element methods are rather in good agreement about the current range value.

At last, the machine is studied at nominal speed, for nominal voltage supply (220 V per phase, 1430 rpm). The

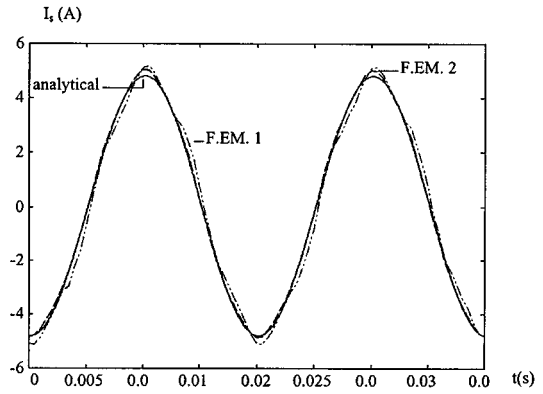

Fig. 8. Stator currents at no load for nominal voltage supply: comparison between analytical approach (—) and FEM computations, with (– · – · 1) and without (- - - 2) rotor bar conductivity.

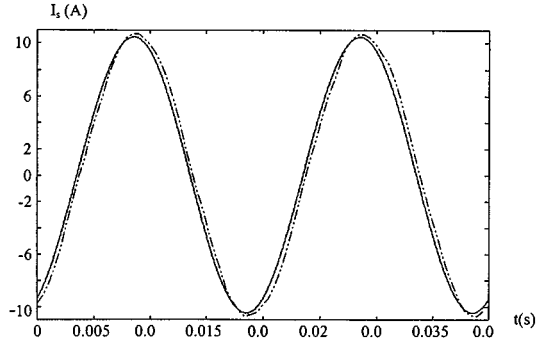

Fig. 9. Stator currents at nominal speed for nominal voltage supply: comparison between FEM computation (– ·· – ·· –) and analytical results (—).

results about stator currents given by the extended analytical method and FEM are portrayed in Figure 9.

The results obtained by the both methods well agree, we can note a discrepancy less than 4% between the two results. The electromagnetic torque developed by the motor during this trial has been also computing by the both methods: the FEM uses the Maxwell stress [13] and the analytical approach, the classical formulation (48):

$$C_{\rm em} = p(\phi_{\alpha{\rm s}} i_{\beta{\rm s}} - \phi_{\beta{\rm s}} i_{\alpha{\rm s}}). \quad (48)$$

Figure 10 shows a comparison of the two results; once again, less than 4% of error can be measured between the analytical approach result and the mean value of the FEM one.

7 Conclusion

We propose in this paper a straightforward analytical modeling of an induction machine extended to saturation consideration. Thanks to the saturated permeance concept, analytical approach has been developed. One of the main results of this approach is to show that the inductance parameters depend on the magnetising current value but not on its phase. As a result, the inductance parameter computation is simplified. A method of inductance

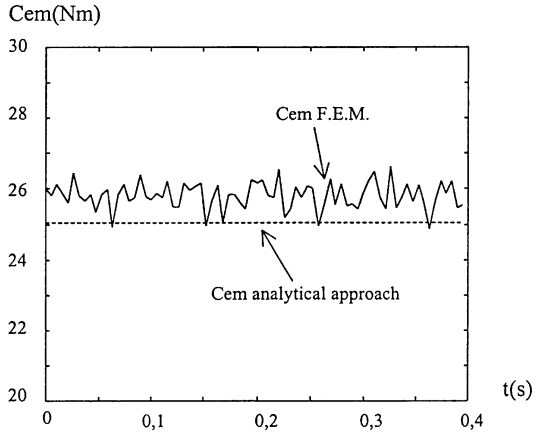

Fig. 10. Electromagnetic torque at nominal speed for nominal voltage supply: comparison between FEM computation (mean value = 25.8 Nm) and analytical results (25 Nm).

computation using finite elements is deduced, as well as the calculation of the transformation ratio. Leakage and dispersion coefficients can also be computed. Then the approach is used to study a nominal voltage fed machine at no load and for nominal speed. The comparison with FEM results are satisfactory, showing the validity of the extended analytical approach at least for this kind of induction machine.

Appendix: Induction machine characterisation

220 V/380 V, 50 Hz,
$p = 2$,
$\mathcal{I} = 0.11$, $D = 104$ mm, $e = 0.3$ mm,
$n_\mathrm{s} = 99$, $n_\mathrm{r} = 1$, $k_\mathrm{s} = 0.92$, $k_\mathrm{r} = 0.24$.

Maximum value of rated magnetising current i_μ: 5.55 A.
$R_\mathrm{s} = 1.896\ \Omega$, $R_\mathrm{r} = 1.29\ \Omega$, $\mathcal{M}_\mathrm{sr} = 0.184$ H for rated magnetising current. These parameters are already referred to stator armature.

References

1. S. Moreau, J.P. Gaubert, P. Coirault, G. Champenois, *Parameter estimation of an induction machine* (Electrimacs, St-Nazaire, 1996), pp. 947–952.
2. S. Williamson, M.J. Robinson, Proc. IEE b **138**, 264 (1991).
3. F. Piriou, A. Razek, IEEE Trans. Mag. **19**, 2628 (1983).
4. B. Semail, F. Piriou, A. Razek, Proc. IEE **282**, 358 (1987).
5. P.M. Leplat, B. Lemaire-Semail, S. Clenet, F. Piriou, Compel **15**, 82 (1996).
6. B. Semail, F. Bouillault, A. Razek, *Consideration of saturation effects in modelling a squirrel cage induction machine used in vector controlled*, I.M.A.C.S. Modeling and contol of electical machines (New Trends, September, 1991), p. 17.
7. N.A. Demerdash, P. Baldassari, IEEE Trans. Energy Conv. **7**, 698 (1992).
8. J.P. Louis, B. Lemaire-Semail, F. Bouillault, *Extension de la méthode de Park à la machine asynchrone en régime saturé en vue d'une modélisation analytique*, G.D.R. Conception de dispositifs et systèmes électrotechniques, Toulouse, 8 juin 1993.
9. T. Kasmieh, Y. Lefevre, X. Roboam, J. Faucher, Eur. Phys. J. AP **1**, 57 (1998).
10. S. Williamson, M.C. Begg, Proc. IEE b **132**, 125 (1985).
11. A. Yahiaoui, F. Bouillault, IEEE Trans. Magn. **30**, 3690 (1994).
12. I. Boldea, S.A. Nasar, Electr. Mach. Pow. Syst. **12**, 195 (1987).
13. A. Razek, J.L. Coulomb, M. Feliachi, J.C. Sabonnadière, IEEE Trans. Mag. **17**, 3250 (1981).
14. A. Kladas, Ph.D. thesis, University Paris VI, LGEP, 1987.